Catalysis Today 164 (2011) 404–409

Contents lists available at ScienceDirect

Catalysis Today

journal homepage: www.elsevier.com/locate/cattod

Photocatalytic mineralization of volatile organic compounds over commercial titanium(IV) oxide modified with rhodium(III) ion under visible light irradiation and correlation between physical properties and photocatalytic activity

Sho Kitano, Keiji Hashimoto, Hiroshi Kominami*

Department of Applied Chemistry, Faculty of Science and Engineering, Kinki University, 3-4-1 Kowakae, Higashiosaka, Osaka 577-8502, Japan

ARTICLE INFO

Article history:
Available online 14 November 2010

Keywords:
Photocatalyst
Visible light
Rhodium ion
TiO_2
Degradation of acetaldehyde
Degradation of acetone

ABSTRACT

Rhodium(III) ion (Rh^{3+})-modified TiO_2 (Rh^{3+}/TiO_2) samples having various physical properties and structures (anatase and rutile) were prepared using commercially available TiO_2 samples. Thus-prepared Rh^{3+}/TiO_2 samples were used for degradation of acetaldehyde or mineralization of acetone with a constant vapor pressure under irradiation of visible light and correlations between the photocatalytic activities and physical properties were investigated. Rhodium(III) ion on the surface of TiO_2 worked as an inorganic photosensitizer and the Rh^{3+}/TiO_2 samples showed a kind of volcano-like tendency against specific surface area of TiO_2, indicating that the balance of surface area and crystallinity of TiO_2 is important in an Rh^{3+}/TiO_2 photocatalyst. The latter reaction system was found to be a simple and convenient method to evaluate the activity of a photocatalyst in a short time. The role of Rh^{3+} as a catalyst for multi-electron reduction of oxygen is discussed on the basis of results obtained for Rh^{3+}-modified rutile-type TiO_2 samples.

1. Introduction

Titanium(IV) oxide (TiO_2) is a semiconductors that works as a highly active photocatalyst [1–3] and it is expected to solve the problem of air pollution in houses with volatile organic compounds (VOC), such as formaldehyde, causing sick house syndrome [4]. When TiO_2 is irradiated by UV light of which the energy is larger than that of the band gap, electrons in the valence band are excited to the conduction band, generating holes in the valence band. However, since the amount of UV light in our living spaces is limited, the photocatalytic performance of TiO_2 is insufficiently utilized. Therefore, many efforts have been devoted to synthesis of photocatalysts that respond to visible light [5–12]. We previously reported a new TiO_2-based photocatalyst that responds visible light [13,14]. The photocatalyst, rhodium ion (Rh^{3+})-modified TiO_2 was prepared simply by using the equilibrium adsorption method followed only by filtration and drying (not by thermal activation). In that study, TiO_2 samples having various physical properties were synthesized using HyCOM (hydrothermal crystallization in organic media) [15], which is one of the solvothermal methods, and subsequent calcinations at various temperatures [16]. The Rh^{3+}-modified HyCOM-TiO_2 samples showed photoabsorption in the visible light region probably because Rh^{3+} on the surface of TiO_2 worked as inorganic photosensitizer [17], and the samples exhibited higher levels of activity than the activities of Cu^{2+}-modified HyCOM-TiO_2 samples and nitrogen-doped TiO_2 sample for photocatalytic degradation of 2-propanol under visible light irradiation [14]. Another important finding is that the photocatalytic activity of Rh^{3+}-modified HyCOM-TiO_2 samples was dependent on the physical properties of HyCOM-TiO_2. Since the physical properties of TiO_2 have an influence on various processes, such as adsorption and oxidation of a substrate(s) and further chemical reaction on the surface of TiO_2, and affect the total photocatalytic activity, control of the physical properties of TiO_2 is important for enhancement of photocatalytic activity. The Rh^{3+}-modified HyCOM-TiO_2 samples showed a kind of volcano-like tendency against calcination temperature, suggesting that the balance of surface area and crystallinity of TiO_2 is important in an Rh^{3+}-modified HyCOM-TiO_2 photocatalyst. We were interested in whether this tendency can be seen for Rh^{3+}-modified TiO_2 samples other than Rh^{3+}-modified HyCOM-TiO_2 samples. There are many kinds of commercial TiO_2 samples for photocatalysts that have various physical properties and crystal structures. Therefore, in this study, Rh^{3+}-modified TiO_2 (Rh^{3+}/TiO_2) samples having various physical properties were prepared using commercially available TiO_2 samples. Thus-prepared Rh^{3+}/TiO_2 samples were used for degradation of gaseous acetaldehyde under irradiation of visible light, and correlations between the photocatalytic activities and physical properties were investigated. A simple and convenient method for evaluation of the photocatalytic activity of various Rh^{3+}/TiO_2 samples was also developed.

---

* Corresponding author. Tel.: +81 6 6721 2332; fax: +81 6 6727 2024.
E-mail address: hiro@apch.kindai.ac.jp (H. Kominami).

0920-5861/$ – see front matter © 2010 Elsevier B.V. All rights reserved.
doi:10.1016/j.cattod.2010.10.064

2. Experimental

2.1. Sample preparation

All of the chemicals were used as received without further purification. HyCOM-TiO_2 powder was synthesized by a procedure reported previously [15]. Titanium(IV) butoxide (25 g) in toluene (70 cm^3) was heated at 300 °C for 2 h in an autoclave in the presence of water (10 cm^3) fed in a space separated from alkoxide solution. The resulting powders were washed repeatedly with acetone and dried in air at ambient temperature. Rutile-type TiO_2 powder (MT-150A) was supplied from TAYCA. The HyCOM-TiO_2 powder and the rutile-type TiO_2 powder were calcined at various temperatures in a box furnace for 1 h.

HyCOM-TiO_2 and rutile-type TiO_2 samples calcined at various temperatures and commercial TiO_2 were modified with Rh^{3+} by using the equilibrium adsorption method. Each sample was added to an aqueous solution of rhodium(III) chloride, the amount of which corresponded to 0.2 wt% modification of metal, and stirred and heated in a water bath at ca. 85 °C. Then the suspension was filtered and the filter cake was dried *in vacuo* for 1 h. The amount of Rh^{3+} fixed on TiO_2 was determined by analysis of Rh^{3+} in the filtrate using inductively coupled plasma atomic emission spectroscopy (ICP-AES, Shimadzu ICPS-7500). Hereafter, calcined HyCOM-TiO_2 and rutile-type TiO_2 are designated as Hy(T) and R(T), respectively, where T means calcination temperature in degrees Celsius; for example, the HyCOM-TiO_2 sample calcined at 550 °C is shown as Hy(550). Modified TiO_2 is shown as Rh^{3+}/Hy(550), which means Hy(550) modified with Rh^{3+}.

2.2. Characterization

Powder X-ray diffraction (XRD) was measured using Cu Kα radiation by a Rigaku MultiFlex equipped with a carbon monochromator. The crystallite size of samples was calculated from the half-height width of the 1 0 1 diffraction peak of anatase and the 1 1 1 diffraction peak of rutile using the Scherrer equation; the value of the shape factor, K, was arbitrarily taken to be 0.9. Specific surface area (S_{BET}) of the samples was obtained using the Brunauer–Emmett–Teller (BET) single-point method on the basis of nitrogen (N_2) uptake measured at −196 °C using a Shimadzu Flowsorb 2300. Diffuse reflectance spectra were measured using a Shimadzu UV-2400 UV–Vis spectrometer equipped with a diffuse reflectance measurement unit (ISR-2000) and recorded after Kubelka–Munk analysis.

2.3. Photocatalytic mineralization of acetaldehyde under irradiation of visible light

A sample (100 mg) was suspended in a small amount of distilled water and then the powder was spread on a glass filter (GF-75, 55 mm in diameter, Advantec) with a Buchner funnel under suction. The glass filter together with the sample was dried *in vacuo* for 1 h. A glass filter together with the sample was placed in a separable flask (reactor) as shown in Fig. 1. Before photocatalytic mineralization of acetaldehyde, pretreatment was performed in order to remove organic residue previously adsorbed on the surface of the photocatalyst [10]. The gas phase in the system was replaced with artificial air (oxygen (O_2) (20%)–nitrogen (N_2) gas mixture) and then the photocatalyst was photoirradiated by visible or UV light. The visible and UV light sources in the pretreatment were a 500 W xenon (Xe) lamp (Ushio, SX-UI501-1) with a Y-43 cut filter (Asahi Technoglass) and a 10 W black light (Toshiba, FL10BLB-A, maximum energy at 350 nm). The light intensities of visible light and UV light on the surface of the glass filter were 130 mW cm^{-2} (400–600 nm) and 2 mW cm^{-2}, respectively. Irradiation the Rh^{3+}-modified TiO_2 samples with UV light did not alter the absorption properties of the samples. After complete removal of the organic residue from the photocatalyst, the gas phase in the system was replaced with artificial air again and then 20 μmol of gaseous acetaldehyde was injected in the reactor in the dark. Irradiation of visible light was started after the gas concentration had become constant, with acetaldehyde having reached an adsorption equilibrium in the reactor. A Xe lamp with a Y-43 cut filter was used as the source of visible light in the photocatalytic reaction of the same intensity as that stated above. The amounts of acetaldehyde and CO_2 were determined by using a Shimadzu GC-8A gas chromatograph with a Porapack Q column and a Shimadzu GC-14B gas chromatograph with a polyethylene glycol 20 M column, respectively.

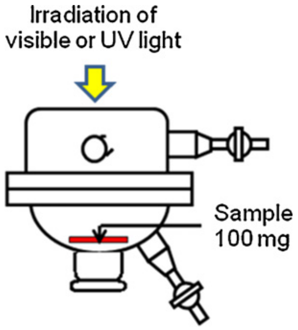

Fig. 1. Reactor used for pretreatment and photocatalytic decomposition of acetaldehyde.

2.4. Photocatalytic mineralization of acetone with constant concentration in gas phase under irradiation of visible light

A sample (100 mg) was fixed on a glass filter by the same method as that described above. A glass vessel containing an aqueous solution of acetone (1 vol%) was connected to the bottom of the reactor, and a glass filter together with the sample was placed in the reactor as shown in Fig. 2. The gas phase in the system was replaced with artificial air, and acetone was gradually evaporated and then the vapor was saturated in the reactor overnight. After adsorption of acetone had reached an equilibrium, the photocatalyst was irradiated by visible light of a Xe lamp with a Y-43 cut filter, the intensity on the surface of the glass filter being 150 mW cm^{-2} (400–600 nm). The amounts of acetone and CO_2 were determined by the same method as that stated above.

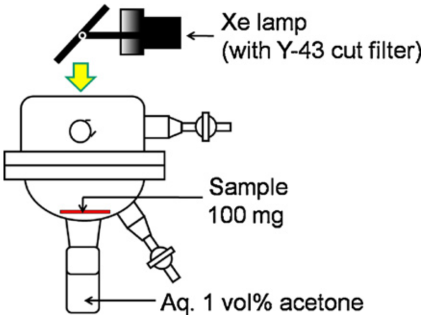

Fig. 2. Reactor used for photocatalytic decomposition of acetone with a constant vapor pressure.

3. Results and discussion

3.1. Complete oxidation of acetaldehyde by Rh^{3+}/Hy(550) under visible light irradiation

In this study, acetaldehyde was chosen as a model volatile organic compound because it is one of the main pollutants in houses. To evaluate whether the Rh^{3+}/TiO_2 photocatalyst has the ability to mineralize acetaldehyde (completely decompose acetaldehyde to CO_2), Rh^{3+}/Hy(550) was used in this reaction system. Fig. 3 shows the time course of the amount of CO_2 formed from acetaldehyde (initially 20 μmol). The amount of CO_2 increased just after irradiation of visible light, and reaction rate (the slope of the formation curve) gradually decreased. Totally, 40 μmol of CO_2 was formed after irradiation for 15 h. The amount of CO_2 was in good agreement with the stoichiometry of the amount of initial acetaldehyde, indicating that photocatalytic mineralization of acetaldehyde occurred under irradiation of visible light according to Eq. (1) without formation of other persistent intermediates [18].

$$CH_3CHO + 5/2O_2 \rightarrow 2CO_2 + 2H_2O \quad (1)$$

Therefore, these results indicate that Rh^{3+}/Hy(550) has the ability to mineralize acetaldehyde under irradiation of visible light. When a bare TiO_2 (Hy(550)) was used for this reaction system, only a small amount of CO_2 was detected probably due to very weak UV light slipping from the Y-43 cut filter. However, the rate of CO_2 formation (0.35 $\mu mol\,h^{-1}$) was much smaller than the initial rate for the Rh^{3+}/Hy(550) (7.3 $\mu mol\,h^{-1}$) and therefore, the rate for bare Hy(550) can be neglected in the present system.

3.2. Correlation of physical properties of commercial TiO_2 and photocatalytic activity of Rh^{3+}/TiO_2 under visible light irradiation

There are many kinds of commercial TiO_2 samples for photocatalyst use that have various physical properties and crystal structures. Using commercially available TiO_2 samples, Rh^{3+}-modified TiO_2 samples having various physical properties were prepared and were used for mineralization of acetaldehyde under irradiation of visible light. Table 1 summarizes the physical properties of commercial TiO_2 samples used in this study, indicating that effects of physical properties on photocatalytic activity of Rh^{3+}-modified TiO_2 samples were investigated in a wide range. For comparison, data of Hy(550) and Hy(700) are also shown in Table 1. Since excess loading of Rh^{3+} on TiO_2 samples causes various complex results, the amount of Rh^{3+} was fixed at 0.2 wt%, which enabled good dispersion of Rh^{3+} in all samples. Fig. 4(a) and (b) shows diffuse reflection spectra of these TiO_2 samples before and after modification with Rh^{3+}, respectively. Absorption in the visible light region was observed in all of the modified samples prepared

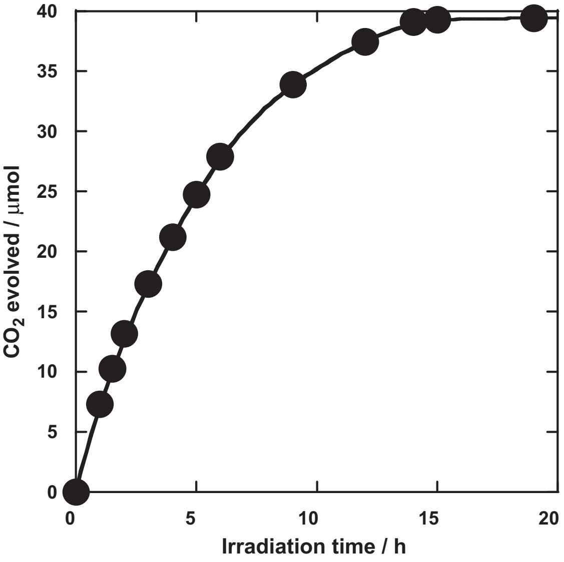

Fig. 3. Time course of CO_2 formation from 20 μmol of acetaldehyde.

Table 1
Physical properties of commercial TiO_2.

TiO_2	d^a (nm)	S_{BET} ($m^2\,g^{-1}$)	Phase^b
Hy(550)	14 (A)	81	A
Hy(700)	29 (A)	35	A
P 25	22 (A)	54	A, R
ST-01	7 (A)	253	A
MT-150A	15 (R)	93	R
F-6	12 (A)	98	A, R
TNT^c	11 (A)	184	A

[a] Crystalline size of anatase and rutile.
[b] A: anatase, R: rutile.
[c] TNT: titania nanotube supplied from Prof. Ohno (Kyushu Institute of Technology).

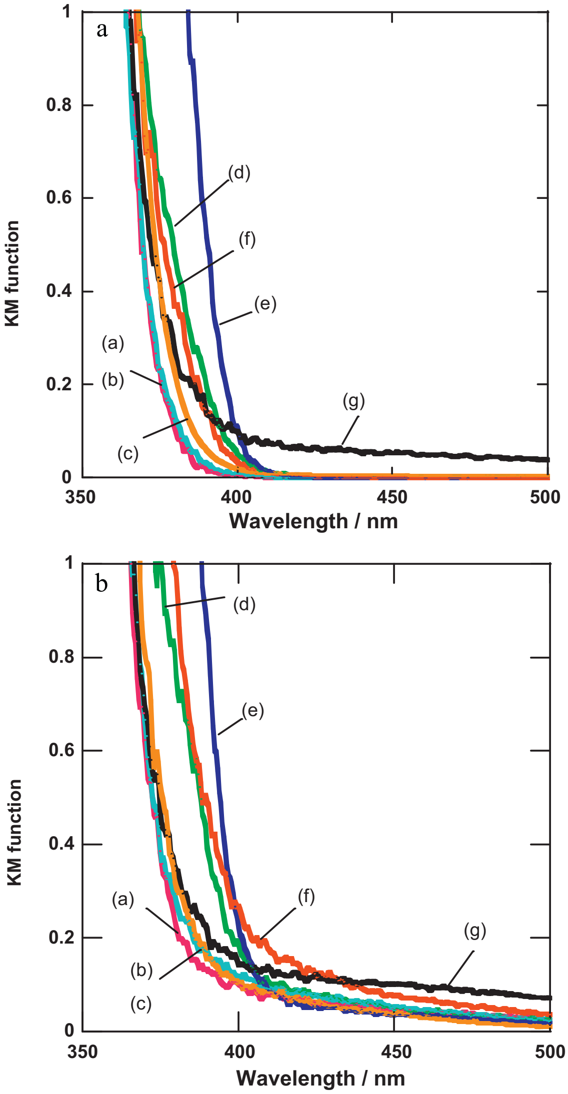

Fig. 4. a: Diffuse reflection spectra of bare commercial TiO_2: (a) Hy(550), (b) Hy(700), (c) P 25, (d) ST-01, (e) MT-150A, (f) F-6 and (g) TNT. **b**: Diffuse reflection spectra of commercial TiO_2 modified with Rh^{3+}: (a) Hy(550), (b) Hy(700), (c) P 25, (d) ST-01, (e) MT-150A, (f) F-6 and (g) TNT.

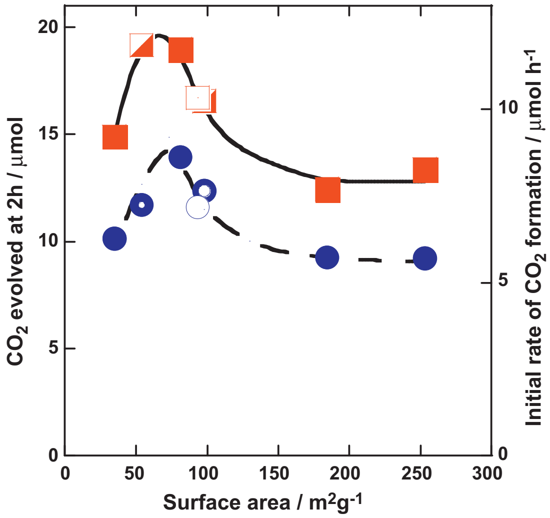

Fig. 5. Evolution of CO_2 for 2 h (squares) and initial rate of CO_2 formation (circles) over Rh^{3+}/TiO_2 having different surface areas: anatase-type TiO_2 (closed), rutile-type TiO_2 (open), anatase and rutile-type TiO_2 (half-closed).

in this study, indicating that modification with Rh^{3+} was effective for visiblization of TiO_2 independent of the physical properties and the crystalline form of TiO_2.

Thus-prepared Rh^{3+}/TiO_2 samples having various physical properties were used for mineralization of acetaldehyde under irradiation of visible light. It was confirmed that organic contaminants adsorbed on photocatalysts were almost completely removed in all samples when they were pretreated with UV light for 45 h. All samples showed a time course of CO_2 formation similar to that of Rh^{3+}/Hy(550) shown in Fig. 3. Two values, the initial reaction rate of CO_2 formation (r_0) and the amount of CO_2 formed during 2-h irradiation (Y_{CO_2}), were determined from the time course of CO_2 formation for each Rh^{3+}/TiO_2 sample in order to compare the photocatalytic activities. These values are plotted against the specific surface area of each sample in Fig. 5. A kind of volcano-like tendency against specific surface area was observed in both cases, and almost the same peaks at 70 $m^2 g^{-1}$ in the two plots indicate that the two values (r_0 and Y_{CO_2}) can be used as indicators of photocatalytic activity of Rh^{3+}-modified TiO_2 samples. Fig. 5 clearly shows that the Rh^{3+}/TiO_2 sample using TiO_2 with a specific surface area of about 70 $m^2 g^{-1}$ exhibited the highest level of activity for mineralization of acetaldehyde under irradiation of visible light. We have reported that HyCOM-TiO_2 samples modified with Rh^{3+} showed a kind of volcano-like tendency against calcination temperature and that photocatalytic activity of the samples was dependent on the physical properties of HyCOM-TiO_2. The specific surface area of TiO_2 affects adsorption of the substrate and the crystallinity affects the amount of defects, career mobility and electron–hole recombination probability. Therefore, these two properties are important factors for a higher level of photocatalytic activity. In the present study, various TiO_2 samples having different crystal structures, i.e., anatase, rutile and a mixture of these two, were used. However, Fig. 5 shows that the crystal structure of TiO_2 had no effect on photocatalytic activity of Rh^{3+}/TiO_2 samples. These results also indicate that the balance of specific surface area and crystallinity is important regardless of whether TiO_2 samples are synthesized commercially or made in a laboratory.

3.3. *Evaluation of photocatalytic activity of various Rh^{3+}/TiO_2 samples using a simple and convenient method*

In the mineralization of acetaldehyde, pretreatment of the photocatalyst with photoirradiation of visible or UV light was performed in order to precisely evaluate photocatalytic activity because the surface of a photocatalyst is always contaminated with some organic species other than the substrate (acetaldehyde in this study) and stoichiometry of photocatalytic mineralization such as Eq. (1) was not confirmed. Therefore, a simple and convenient method to evaluate photocatalytic activity is required. In this study, a new method, i.e., photocatalytic mineralization of acetone with a constant vapor pressure, was developed and the photocatalytic activity of Rh^{3+}/TiO_2 samples was evaluated in a short time using this method (in the previous system, at least 45 h of irradiation time was needed as pretreatment.) In this system, acetone in the glass vessel connected at the bottom of the separable flask evaporates and the vapor is saturated in the reactor. When acetone in gas phase is consumed for photocatalytic reaction on the surface of the photocatalyst under irradiation, acetone in the aqueous solution is supplied to the gas phase, keeping the acetone concentration in the gas phase almost constant. Thus, photocatalytic reaction in the present system proceeds under the condition in which an adsorption equilibrium of acetone is attained. In actual living spaces, VOC are emitted to the gas phase and adsorbed on walls in the room at any time. Since the conditions of the present system are similar to those of actual living spaces, the performance of photocatalysts in practical use can be estimated in a short time. In this method, photocatalytic activity for oxidative decomposition of both organic contaminants and acetone is evaluated. However, the amount of organic contaminants is much smaller than that of acetone and has almost no effect on decomposition of acetone. Fig. 6 shows time courses of CO_2 formed in the present system by Rh^{3+}/Hy(550) and Rh^{3+}/R(300) under irradiation of visible light. As shown in Fig. 6, CO_2 formed linearly with irradiation time in both cases, indicating zero-order kinetics probably due to saturation of substrates to be decomposed in this condition. Therefore, photocatalytic activity was easily evaluated from the rate of CO_2 formation within only 5 h without long pretreatment. We noted that the Rh^{3+}/R(300) sample exhibited almost the same reaction rate without catalyst deactivation as that of the Rh^{3+}/Hy(550) sample. In the Rh^{3+}-modified TiO_2 photocatalyst, Rh^{3+} on the surface of TiO_2 is excited under irradiation of visible light and injects electrons into the conduction band of TiO_2 [17,19,20]. Thus-formed Rh species having a higher oxidation state receives electrons from the substrates, i.e., oxidizes

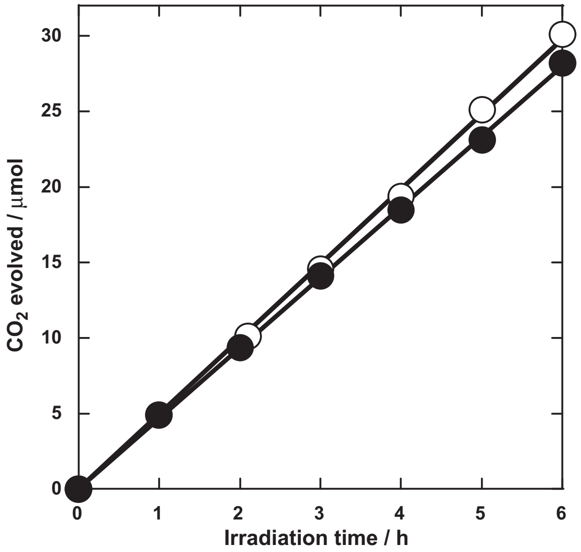

Fig. 6. Time courses of CO_2 formation in decomposition of acetone with a constant vapor pressure by Rh^{3+}-modified anatase-type (open circles) and rutile-type (closed circles) TiO_2.

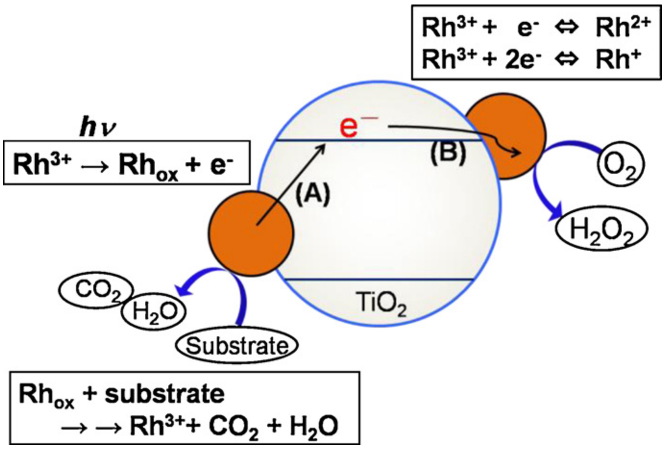

Fig. 7. Speculated scheme of electron transfer and role of Rh species in Rh^{3+}/TiO_2.

substrates, and returns to the initial state. Since electrons injected into the conduction band of TiO_2 should be consumed by O_2 for continuous photocatalytic reaction, potential of the conduction band is very important. Rutile-type TiO_2 has the bottom of the conduction band at 0 V vs. SHE [21], which is slightly positive to the potential of one-electron reduction of O_2 ($O_2 + H^+ + e^- = HO_2$, −0.046 V vs. SHE). Therefore, one-electron reduction of O_2 does not occur in rutile TiO_2. On the other hand, one-electron reduction of O_2 does occur in anatase-type TiO_2 because of its sufficient potential of the conduction band at −0.2 V vs. SHE [22]. Therefore, it is generally accepted that rutile-type TiO_2 exhibits very low level of activity in photocatalytic oxidation of organic compounds in the presence of O_2 under irradiation of UV light because the photogenerated electrons are accumulated in TiO_2. In fact, bare rutile-type TiO_2 showed lower photocatalytic activity than that of bare anatase-type TiO_2 in mineralization of acetone under irradiation of UV light and the amount of CO_2 formed gradually decreased in the case of rutile-type TiO_2, although the results are not shown. Electrons in the conduction band should be consumed for continuous reaction in both cases, i.e., Rh^{3+}/R(300) under visible light irradiation and bare R(300) under UV light irradiation. The comparable activity of Rh^{3+}/R(300) to that of Rh^{3+}/Hy(550) under visible light irradiation despite insufficient potential of the conduction band for a one-electron reduction of O_2 suggests that multi-electron reduction of O_2 occurred in the Rh^{3+}/TiO_2 system. Since the redox potentials of Rh^{3+} ($Rh^{3+} + e^- = Rh^{2+}$, $E = 0.158$ V; $Rh^{3+} + 2e^- = Rh^+$, $E = 0.158$ V) are more negative than those of multi-electron reduction of O_2 (two-electron reduction: $O_2 + 2H^+ + 2e^- = H_2O_2$, $E = 0.68$ V; or four-electron reduction: $O_2 + 4H^+ + 4e^- = 2H_2O$, $E = 1.23$ V), Rh^{3+} is a strong candidate as a catalyst for multi-electron reduction of O_2. The role of Rh^{3+} as a catalyst for multi-electron reduction of O_2 is as follows: some of the Rh^{3+} loaded on the surface of TiO_2 was reduced by electrons in the conduction band [19] and the reduced Rh species was oxidized to Rh^{3+} through multi-electron reduction of O_2. The assumed mechanism of mineralization of organic compounds over Rh^{3+}/TiO_2 under irradiation of visible light is shown in Fig. 7. Under visible light irradiation, Rh^{3+} injects electrons into the conduction band of TiO_2 (electron transfer (A) indicated in Fig. 7). The Rh species having a higher oxidative state oxidizes organic substrates and returns to the initial state. The electrons injected to the conduction band move and are accepted by other Rh^{3+} (electron transfer (B) indicated in Fig. 7). The reduced Rh species are oxidized through multi-electron reduction of O_2. Therefore, the photoexcited Rh^{3+} works as an electron donor, while the other Rh^{3+} species act as electron accepters.

Table 2
Specific surface area of uncalcined and calcined rutile-type TiO_2.

T_{cal}[a] (°C)	S_{BET} ($m^2\,g^{-1}$)
Uncalcined	93
200	82
300	56
550	40
700	27
900	10

[a] Calcination temperature.

3.4. Effect of physical properties of rutile-type TiO_2 on photocatalytic activity of Rh^{3+}/TiO_2 under visible light irradiation

It was found that photocatalytic activity of Rh^{3+}/TiO_2 samples was dependent on the specific surface area and crystallinity but independent of structure of TiO_2 and that Rh^{3+}/R(300) exhibited photocatalytic activity continuously in contrast to bare R(300). Correlations between physical properties and photocatalytic activity of Rh^{3+}/TiO_2 under irradiation of visible light were further

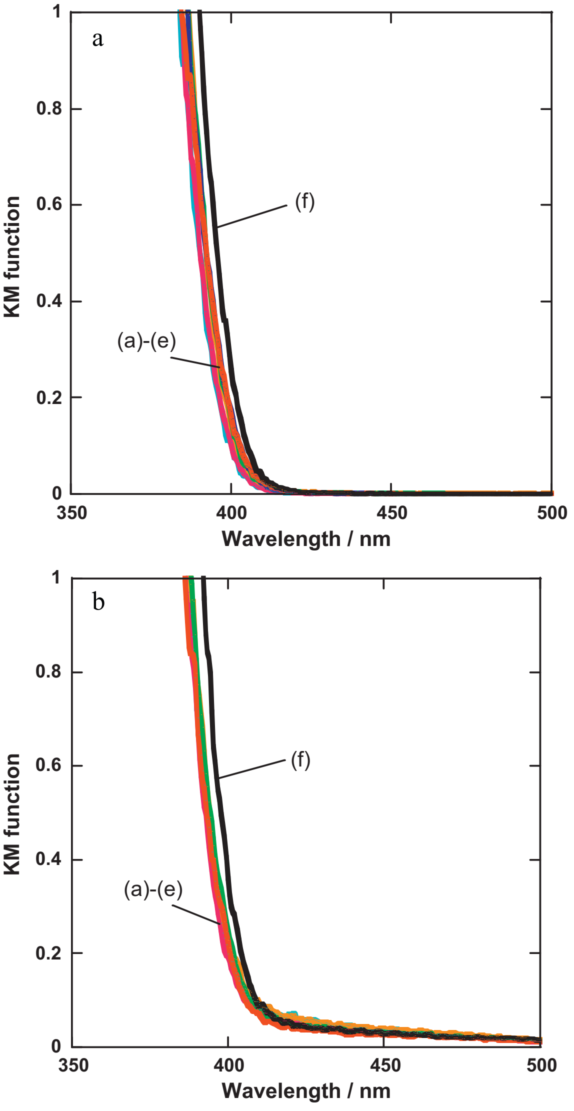

Fig. 8. **a**:Diffuse reflection spectra of rutile-type TiO_2 samples (a) uncalcined and calcined at (b) 200 °C, (c) 300 °C, (d) 550 °C, (e) 700 °C and (f) 900 °C. **b**: Diffuse reflection spectra of Rh^{3+}/rutile-type TiO_2 samples (a) uncalcined and calcined at (b) 200 °C, (c) 300 °C, (d) 550 °C, (e) 700 °C and (f) 900 °C.

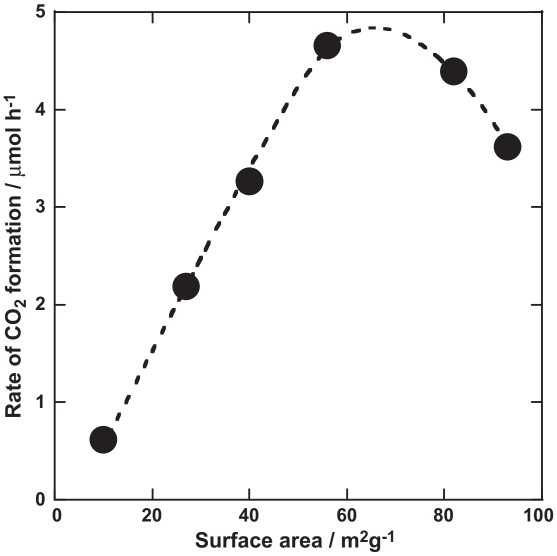

Fig. 9. Rate of CO_2 formation from acetone over Rh^{3+}/rutile-type TiO_2 with different surface areas prepared by calcination at various temperatures.

investigated using rutile-type TiO_2. The specific surface areas of rutile-type TiO_2 samples calcined at various temperatures are shown in Table 2. The specific surface area of rutile-type TiO_2 decreased with increase in the calcination temperature. Fig. 8(a) shows diffuse reflection spectra of rutile-type TiO_2 samples calcined at various temperatures. Calcination did not alter the photoabsorption property of rutile-type TiO_2 samples. The amounts of Rh^{3+} loaded on rutile-type TiO_2 samples were 0.2 wt% in all samples. Fig. 8(b) shows diffuse reflection spectra of Rh^{3+}-modified rutile-type TiO_2 samples. As was seen in Rh^{3+}-modified TiO_2 samples (Fig. 4(b)), absorption in the visible light region was observed in all of the modified rutile-type TiO_2 samples, indicating that visiblization of rutile-type TiO_2 with Rh^{3+} was insensitive to the physical properties.

The photocatalytic activity of Rh^{3+}-modified rutile-type TiO_2 samples was evaluated by using mineralization of acetone with a constant vapor pressure under irradiation of visible light. Fig. 9 shows the effect of specific surface area of rutile-type TiO_2 on the rate of CO_2 formation. The Rh^{3+}-modified rutile-type TiO_2 samples also exhibited a kind of volcano-like tendency in photocatalytic activity, i.e., the Rh^{3+}/R(300) sample using TiO_2 with a specific surface area of around 65 m^2 g^{-1} exhibited the highest level of activity. Therefore, in the case of rutile-type TiO_2, the balance of specific surface area and crystallinity of TiO_2 is important in an Rh^{3+}/TiO_2 photocatalyst.

4. Conclusions

A rhodium(III) ion-modified TiO_2 (Rh^{3+}/TiO_2) photocatalyst decomposed acetaldehyde completely under irradiation of visible light. In photocatalytic degradation of acetaldehyde, Rh^{3+}-modified commercial TiO_2 samples having various properties showed a kind of volcano-like tendency against specific surface area of TiO_2 regardless of the structure of TiO_2 (anatase and rutile), and the sample having a specific surface area of ca. 70 m^2 g^{-1} exhibited the highest level of activity. These results indicate that the balance of specific surface area and crystallinity is important in Rh^{3+}/TiO_2.

A new method, i.e., photocatalytic mineralization of acetone with a constant vapor pressure, was developed and the photocatalytic activity of Rh^{3+}/TiO_2 samples was evaluated in a short time using this method. The Rh^{3+}-modified rutile-type TiO_2 samples exhibited almost the same photocatalytic activity as that of the Rh^{3+}-modified anatase-type TiO_2 sample. The results suggested that Rh^{3+} on the surface of TiO_2 worked as a catalyst for multi-electron reduction of oxygen.

Acknowledgements

This work was partly supported by a fund (Project No. P07020) from the Environmental Technology Development Department of New Energy and Industrial Technology Development Organization (NEDO). One of the authors (H.K.) is also grateful for financial support from the Faculty of Science and Engineering, Kinki University. We are grateful to Professor Teruhisa Ohno (Kyushu Institute of Technology) for the gift of titania nanotube.

References

[1] S. Matsuda, A. Kato, Appl. Catal. 8 (1983) 149.
[2] M. Inomata, A. Miyamoto, Y. Murakami, J. Chem. Soc., Chem. Commun. (1980) 233.
[3] F. Luck, Bull. Soc. Chim. Belg. 100 (1991) 781.
[4] R.M. Hoffmann, T.S. Martin, W. Choi, W.D. Bahnemann, Chem. Rev. 95 (1995) 69.
[5] S. Sato, Chem. Phys. Lett. 123 (1986) 126.
[6] R. Asahi, T. Morikawa, T. Ohwaki, K. Aoki, Y. Taga, Science 293 (2001) 269.
[7] T. Ohno, M. Akiyoshi, T. Umebayashi, K. Asai, T. Mitui, M. Matsumura, Appl. Catal. A 265 (2004) 115.
[8] R. Abe, H. Takami, N. Murakami, B. Ohtani, J. Am. Chem. Soc. 130 (2008) 7780.
[9] H. Irie, S. Miura, K. Kamiya, K. Hashimoto, Chem. Phys. Lett. 457 (2008) 202.
[10] H. Irie, K. Kamiya, T. Shibanuma, S. Miura, D.A. Tryk, T. Yokoyama, K. Hashimoto, J. Phys. Chem. C 113 (2009) 10761.
[11] H. Yu, H. Irie, K. Hashimoto, J. Am. Chem. Soc. 130 (2008) 7780.
[12] H. Kisch, L. Zang, C. Lange, W.F. Maier, C. Antonius, D. Meissner, Angew. Chem. Int. Ed. Engl. 37 (1998) 3034.
[13] S. Kitano, K. Hashimoto, H. Kominami, Chem. Lett. 39 (2010) 627.
[14] S. Kitano, K. Hashimoto, H. Kominami, Appl. Catal. B: Environ., in press, doi:10.1016/j.apcatb.2010.09.021.
[15] H. Kominami, M. Kohno, Y. Takada, M. Inoue, T. Inui, Y. Kera, Ind. Eng. Chem. Res. 38 (1999) 3925.
[16] H. Kominami, S.-y. Murakami, J.-i. Kato, Y. Kera, B. Ohtani, J. Phys. Chem. B 106 (2002) 10501.
[17] Z. Dai, G. Burgeth, F. Parrino, H. Kisch, J. Organomet. Chem. 694 (2009) 1049.
[18] T. Arai, M. Yanagida, Y. Konishi, Y. Iwasaki, H. Sugihara, K. Sayama, J. Phys. Chem. C 111 (2007) 7574.
[19] N. Murakami, T. Chiyoya, T. Tsubota, T. Ohno, Appl. Catal. A 348 (2008) 148.
[20] H. Irie, T. Shibanuma, K. Kamiya, S. Miura, T. Yokoyama, K. Hashimoto, Appl. Catal. B 96 (2010) 142.
[21] H.P. Maruska, A.K. Ghosh, Sol. Energy 20 (1978) 443.
[22] T. Torimoto, N. Nakamura, S. Ikeda, B. Ohtani, Phys. Chem. Chem. Phys. 4 (2002) 5910.